Predictive Value of ^{99m}Tc-MAA SPECT for ^{90}Y-Labeled Resin Microsphere Distribution in Radioembolization of Primary and Secondary Hepatic Tumors

Harun Ilhan[1], Anna Goritschan[1], Philipp Paprottka[2], Tobias F. Jakobs[3], Wolfgang P. Fendler[1], Andrei Todica[1], Peter Bartenstein[1], Marcus Hacker[1,4], and Alexander R. Haug[1,4]

[1]*Department of Nuclear Medicine, University of Munich, Munich, Germany;* [2]*Institute of Clinical Radiology, University of Munich, Munich, Germany;* [3]*Department of Diagnostic and Interventional Radiology, Krankenhaus Barmherzige Brüder, Munich, Germany; and* [4]*Division of Nuclear Medicine, Department of Biomedical Imaging and Image-Guided Therapy, University of Vienna, Vienna, Austria*

This study analyzed the predictive value of ^{99m}Tc-labeled macroaggregated albumin (^{99m}Tc-MAA) SPECT for ^{90}Y-labeled resin microsphere therapy (radioembolization) by comparing uptake on pretherapeutic ^{99m}Tc-MAA SPECT with uptake on posttherapeutic ^{90}Y-bremsstrahlung SPECT. **Methods:** We included 502 patients (55% male; mean age ± SD, 62 ± 11 y) who underwent radioembolization between 2005 and 2013 because of primary or secondary liver malignancies (colorectal cancer [n = 195, 38.8%], neuroendocrine tumors [n = 77, 15.3%], breast cancer [n = 68, 13.5%], hepatocellular carcinoma [n = 59, 11.8%], cholangiocellular carcinoma [n = 40, 8.0%], or urologic tumors [n = 14, 2.8%]). Manually drawn regions of interest around tumors and adjacent healthy liver tissue for up to 3 lesions per patient on ^{99m}Tc-MAA and ^{90}Y-bremsstrahlung scans were used to quantify mean counts per pixel and evaluate the mean tumor-to-background ratio (TBR). Data were given as mean ± SD. Additionally, uptake in lesions on ^{99m}Tc-MAA and ^{90}Y-bremsstrahlung scans was graded visually as homogeneously higher than (grade 1), heterogeneously higher than (grade 2), equal to (grade 3), or lower than (grade 4) uptake in normal liver tissue. The Mann–Whitney *U* test and Spearman correlation were used to evaluate statistically significant differences between ^{99m}Tc-MAA and ^{90}Y-bremsstrahlung SPECT. **Results:** In total, 1,008 lesions were analyzed. Of the 23% (230/1,008) of lesions that had grade 1 uptake on ^{99m}Tc-MAA SPECT, 81% (186/230) remained grade 1 after radioembolization whereas 16% (37/230) were grade 2. Of the lesions with grade 2 uptake on ^{99m}Tc-MAA SPECT, 16% had grade 1 uptake and 82% grade 2 uptake after radioembolization. Of the lesions with grade 3 uptake, however, 27% had grade 1 uptake and 47% grade 2 uptake after radioembolization. Even among the lesions with grade 4 uptake on ^{99m}Tc-MAA SPECT, 21% had grade 1 uptake and 46% grade 2 uptake after radioembolization. The mean TBR on ^{99m}Tc-MAA and ^{90}Y-bremsstrahlung SPECT showed a significant, though low, correlation in the total population (r = 0.26; $P < 0.001$) and in hepatocellular carcinoma (r = 0.4; $P < 0.001$), cholangiocellular carcinoma (r = 0.3; $P < 0.05$), breast cancer (r = 0.3; $P < 0.001$), colorectal cancer (r = 0.2; $P < 0.001$), and neuroendocrine tumors (r = 0.2; $P < 0.01$). **Conclusion:** Although significant for most lesions, the correlation between ^{99m}Tc-MAA and ^{90}Y-microsphere mean TBR was low. Classifying uptake into 4 grades revealed that lesions with high uptake on ^{99m}Tc-MAA SPECT maintain high uptake within radioembolization. More than 60% of lesions with a pretherapeutically lower uptake than in healthy liver tissue, however, showed high uptake within radioembolization. Patients with low tumor uptake on pretherapeutic ^{99m}Tc-MAA imaging should not be excluded from radioembolization.

Key Words: ^{90}Y radioembolization; liver tumor; SIRT; SPECT/CT; ^{99m}Tc macroaggregated albumin

J Nucl Med 2015; 56:1654–1660
DOI: 10.2967/jnumed.115.162685

Radioembolization with ^{90}Y-labeled microspheres is gaining increasing importance in the therapy of primary and secondary liver tumors. In selected cases such as hepatocellular carcinoma (HCC), hepatically metastasized colorectal cancer (CRC), and neuroendocrine tumors (NETs), radioembolization is included as a therapeutic option in international guidelines although it remains controversial (*1–3*). Even in the less common secondary liver tumors such as pancreatic cancer or malignant melanoma, radioembolization is increasingly used and accompanied by controllable short-term toxicities and encouraging response and survival outcome rates (*4,5*). However, larger study populations with various primary tumors are needed to strengthen the value of radioembolization in the clinical management of patients with primary and secondary liver malignancies. Over the last few years, several study groups have tried to define and objectify the role of ^{99m}Tc-labeled macroaggregated albumin (^{99m}Tc-MAA) uptake on SPECT for radioembolization. Angiography with injection of ^{99m}Tc-MAA serves as an obligatory preliminary assessment for endovascular mapping, detecting hepatic perfusion and—if necessary—allowing interventional coiling of aberrant vessels to avoid dystopic flow of ^{90}Y-microspheres during radioembolization (*6*). In terms of prognostic factors, ^{18}F-FDG PET was able to predict survival after radioembolization in a study of 26 patients with cholangiocellular carcinoma (CCC), whereas high tumor vascularization assessed from data on ^{99m}Tc-MAA angiography before radioembolization was associated with worse prognosis (*7*). This finding remains surprising, as one might assume that high tumor vascularization as depicted in high uptake on ^{99m}Tc-MAA SPECT might be accompanied by high uptake of ^{90}Y-microspheres within radioembolization and thus lead to higher absorbed tumor doses, as shown by Flamen et al. (*8*). However, these contradictory findings might be explained by the different

Received Jun. 25, 2015; revision accepted Aug. 10, 2015.
For correspondence or reprints contact: Alexander R. Haug, Division of Nuclear Medicine, Department of Biomedical Imaging and Image-Guided Therapy, University of Vienna, Währinger Gürtel 18-20, 1090 Vienna, Austria.
E-mail: alexander.haug@meduniwien.ac.at
Published online Aug. 27, 2015.

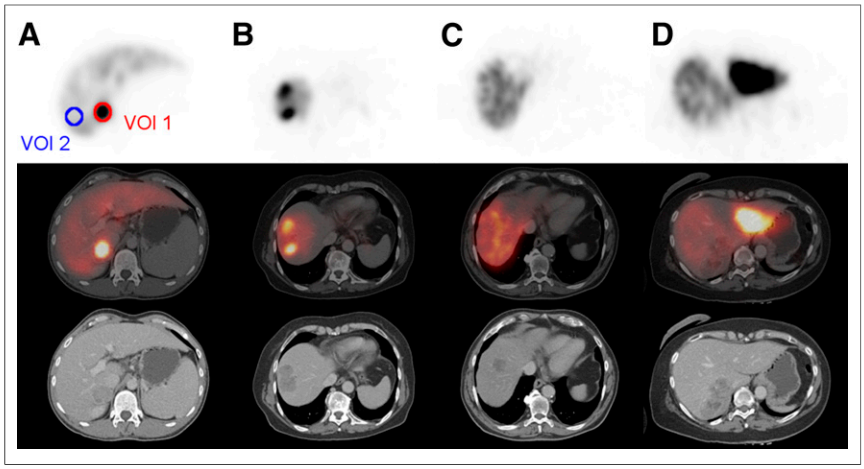

FIGURE 1. Grading of tracer accumulation in ^{99m}Tc-MAA SPECT. (A) Homogenously higher uptake than in normal liver tissue is grade 1. (B) Heterogeneously higher uptake than in normal liver tissue is grade 2. (C) Same uptake as in normal liver tissue is grade 3. (D) Lower uptake than in normal liver tissue is grade 4.

primary tumors (CCC vs. CRC) and the small number of patients (26 vs. 8). Pretherapeutic uptake on ^{99m}Tc-MAA SPECT is often used in the decision-making process for radioembolization and can be relevant to dose calculation as expressed in the partition model (*9*), a multicompartment dosimetric model to determine the therapeutic dose in radioembolization. However, the partition model is more complex than dose calculation methods that are based on empiric data (*10*). The relevance of pretherapeutic imaging is also conferrable to various other tumor primaries. Recently, we reported on ^{99m}Tc-MAA uptake by various tumor entities, including somewhat rare radioembolization indications such as sarcoma (*11*). There was a wide variation in mean tumor-to-background ratio (TBR), with the highest values occurring for NETs, HCC, and CCC, whereas breast cancer, CRC, and sarcoma had the lowest values. The aim of the current study was to compare the uptake pattern of primary and secondary liver tumors on pretherapeutic ^{99m}Tc-MAA SPECT with that on posttherapeutic ^{90}Y-bremsstrahlung SPECT to analyze the ability of the former to predict uptake of ^{90}Y-microspheres.

MATERIALS AND METHODS

Study Population

In total, 502 patients (225 women and 277 men; mean age, 62 ± 11 y; range, 29–91 y) with unresectable primary and metastatic liver malignancies who underwent radioembolization during 2005 and 2013 in our department were retrospectively included in this study. All patients had undergone contrast-enhanced CT or MR imaging and ^{99m}Tc-MAA angiography before radioembolization. Because of the retrospective design of this study, approval was waived by the local ethics committee. All patients provided written informed consent for radioembolization. The patients had hepatic metastases from CRC (n = 195, 39%), NETs (n = 77, 15%), breast cancer (n = 68, 14%), HCC (n = 59, 12%), CCC (n = 40, 8%), urologic tumors (n = 14, 2.8%), pancreatic cancer (n = 13, 2.6%), malignant melanoma (n = 13, 2.6%), gastrointestinal (non-CRC) tumors (n = 10, 2.0%), sarcoma (n = 6, 1.2%), lung cancer (n = 4, 0.8%), or ear-nose-throat tumors (n = 3, 0.6%).

Angiography, Imaging, and Image Analysis

Digital subtraction angiography was performed on all patients for analysis and anatomic mapping of the hepatic arteries and identification of aberrant vessels before radioembolization. During angiography 100 MBq of ^{99m}Tc-MAA (GE Healthcare) were injected into the hepatic artery. Whenever feasible, the right and left hepatic arteries were injected separately to simulate radioembolization. The amount of ^{99m}Tc-MAA was calculated according to the size of the liver lobes, that is, in a typical patient 65 MBq into the right hepatic artery and 35 MBq into the left. Perchlorate (600 mg) was administered orally before angiography to avoid unspecific ^{99m}Tc uptake in the stomach (*12*). One hour after the injection, planar scintigraphy of the abdomen and thorax was performed to quantify the liver–lung shunting fraction. SPECT or SPECT/CT of the abdomen was also performed on all patients.

Radioembolization was performed with ^{90}Y-labeled resin microspheres (SIR-Spheres; SirTex Medical). The ^{90}Y-microspheres were applied directly into the left or right hepatic artery. Three hundred one patients were treated sequentially, and the remaining 201 patients received whole-liver treatment. The applied activity was calculated from percentage tumor burden to the liver and body surface area in 455 patients as expressed in the following formula:

$$\text{Activity (GBq)} = (\text{body surface area} - 0.2) + (\text{tumor volume}/\text{liver volume}).$$

In earlier cases (n = 47), activity was adapted to percentage involvement of the liver (2 GBq if tumor burden < 25%; 2.5 GBq if >25%; 3 GBq if >50%). Planar scintigraphy of the abdomen and thorax and additional SPECT or SPECT/CT of the abdomen were performed 1 h after radioembolization. The patients were examined with a dual-head SPECT camera (e.cam; Siemens Healthcare) or a dual-head SPECT/CT camera (Symbia T; Siemens Healthcare). ^{99m}Tc-MAA and ^{90}Y-bremsstrahlung SPECT were performed on the same camera. ^{99m}Tc-MAA SPECT was performed with low-energy high-resolution collimators (energy window, 140 keV; matrix, 128 × 128; 6° steps; 25 s/frame) and reconstructed using an iterative method (ordered-subsets expectation maximization, 3 iterations, 16 subsets, 1.10 cm in full width at half maximum). ^{90}Y-bremsstrahlung SPECT was performed with medium-energy all-purpose collimators (energy window, 165 keV ± 25%; matrix, 128 × 128; 6° steps; 40 s/frame) and reconstructed using an iterative method (ordered-subsets expectation maximization, 3 iterations, 16 subsets, 1.20 cm in full width at half maximum).

To delineate the liver tumors, the ^{99m}Tc-MAA and ^{90}Y-bremsstrahlung images were coregistered with contrast-enhanced CT or MR images using dedicated software (Hermes Hybrid Viewer; Hermes Medical Solutions). Afterward, regions of interest were drawn manually on up to 3 liver lesions per patient, with a minimum diameter of 15 mm (Fig. 1). The mean counts per pixel were noted. The mean and maximum counts per pixel in healthy liver tissue were noted after a second region of interest had been drawn close to the respective liver lesion to exclude variations due to inhomogeneous ^{99m}Tc-MAA distribution within the liver. Uptake was defined as the mean TBR and calculated by dividing the mean counts per pixel of tumor by the mean counts per pixel of healthy liver tissue.

^{99m}Tc-MAA and ^{90}Y-microsphere uptake was additionally classified into 4 grades, with grade 1 being homogeneous higher uptake in tumor than in normal liver tissue; grade 2, inhomogeneous higher

TABLE 1
Tumor Grade on ^{99m}Tc-MAA and ^{90}Y-Bremsstrahlung SPECT

	^{99m}Tc-MAA			^{90}Y-bremsstrahlung						
	Total			Grade				Total		
Primary	Grade	*n*	%	1	2	3	4	Grade	*n*	%
HCC	1	13	16.9	10	2	1	0	1	17	22.1
	2	58	75.3	7	50	0	1	2	56	72.7
	3	2	2.6	0	2	0	0	3	1	1.3
	4	4	5.2	0	2	0	2	4	3	3.9
CCC	1	14	21.5	13	1	0	0	1	20	30.8
	2	48	73.8	7	40	0	1	2	44	67.7
	3	0	0.0	0	0	0	0	3	0	0.0
	4	3	4.6	0	3	0	0	4	1	1.5
Breast cancer	1	45	36.6	42	2	1	0	1	65	52.8
	2	66	53.7	18	48	0	0	2	53	43.1
	3	2	1.6	2	0	0	0	3	1	0.8
	4	10	8.1	3	3	0	4	4	4	3.3
CRC	1	76	17.2	57	17	1	1	1	102	23.1
	2	338	76.5	37	290	6	5	2	319	72.2
	3	7	1.6	1	4	2	0	3	9	2.0
	4	21	4.8	7	8	0	6	4	12	2.7
NETs	1	57	31.7	49	5	2	1	1	83	46.1
	2	108	60.0	31	76	1	0	2	87	48.3
	3	4	2.2	1	1	2	0	3	7	3.9
	4	11	6.1	2	5	2	2	4	3	1.7
Pancreatic cancer	1	6	25.0	3	3	0	0	1	5	20.8
	2	14	58.3	2	12	0	0	2	16	66.7
	3	0	0.0	0	0	0	0	3	1	4.2
	4	4	16.7	0	1	1	2	4	2	8.3
Lung cancer	1	3	30.0	3	0	0	0	1	3	30.0
	2	7	70.0	0	7	0	0	2	7	70.0
	3	0	0.0	0	0	0	0	3	0	0.0
	4	0	0.0	0	0	0	0	4	0	0.0
Malignant melanoma	1	2	11.1	0	2	0	0	1	2	11.1
	2	15	83.3	2	12	0	1	2	15	83.3
	3	0	0.0	0	0	0	0	3	0	0.0
	4	1	5.6	0	1	0	0	4	1	5.6
Urologic tumor	1	5	16.7	2	3	0	0	1	3	10.0
	2	25	83.3	1	24	0	0	2	27	90.0
	3	0	0.0	0	0	0	0	3	0	0.0
	4	0	0.0	0	0	0	0	4	0	0.0
Ear-nose-throat tumors	1	0	0.0	0	0	0	0	1	2	25.0
	2	8	1000.0	2	4	0	2	2	4	50.0
	3	0	0.0	0	0	0	0	3	0	0.0
	4	0	0.0	0	0	0	0	4	2	25.0
Non-CRC gastrointestinal tumors	1	2	12.5	2	0	0	0	1	6	37.5
	2	13	81.3	4	9	0	0	2	10	62.5
	3	0	0.0	0	0	0	0	3	0	0.0
	4	1	6.3	0	1	0	0	4	0	0.0
Sarcoma	1	7	46.7	5	2	0	0	1	6	40.0
	2	6	40.0	1	4	0	1	2	8	53.3
	3	0	0.0	0	0	0	0	3	0	0.0
	4	2	13.3	0	2	0	0	4	1	6.7

uptake in tumor than in normal liver tissue; grade 3, the same uptake in tumor as in normal liver tissue; and grade 4, lower uptake in tumor than in normal liver tissue (Fig. 1).

Statistical Analysis

Quantitative data are given as mean ± SD and range. The SPSS software package was used for statistical analyses (version 21.0; IBM). After testing for normal distribution of the data using the Kolmogorov–Smirnov test, we tested for significant differences between the TBRs of different tumor entities using the Mann–Whitney *U* test with Bonferroni adjustment for multiple testing. Spearman correlation was used to test for a significant correlation between TBRs from ^{99m}Tc-MAA and ^{90}Y-bremsstrahlung SPECT. A statistically significant difference was defined as that having a *P* value of less than 0.05.

RESULTS

In total, 1,008 liver lesions were analyzed. In previous work we evaluated uptake on ^{99m}Tc-MAA scintigraphy and SPECT within the same patient cohort (*11*). Those results are also included in this analysis (Table 1). Earlier, we could demonstrate that uptake is higher in most liver tumors than in normal liver tissue, being grade 1 in 230 of the 1,008 lesions (22.8%) and grade 2 in 706 (69.2%). Only a minority of lesions had ^{99m}Tc-MAA uptake equal to or lower than that in normal liver tissue (1.5% and 5.7%, respectively). As expected, most of the lesions had concordantly high uptake on ^{90}Y-bremsstrahlung SPECT. Of the 1,008 lesions, 314 (31.2%) had grade 1 uptake, 646 (64.1) grade 2, 19 (1.9%) grade 3, and 29 (2.9%) grade 4. Most lesions with high uptake on ^{99m}Tc-MAA SPECT also had high uptake on ^{90}Y-bremsstrahlung SPECT. Of the 230 lesions with grade 1 uptake before radioembolization, 186 (80.9%) had grade 1, 37 (16.1%) grade 2, 5 (2.2%) grade 3, and 2 (0.9%) grade 4 after radioembolization. Of the 706 lesions with grade 2 uptake on ^{99m}Tc-MAA SPECT, 112 (15.9%) had grade 1, 576 (81.6%) grade 2, 7 (1%) grade 3, and 11 (1.6%) grade 4 on ^{90}Y-bremsstrahlung SPECT. Of the 15 lesions whose uptake equaled that of normal liver tissue on ^{99m}Tc-MAA SPECT (grade 3), 4 (26.7%) were grade 1, 7 (46.7%) grade 2, and 4 (26.7%) grade 3 after radioembolization; no lesion had grade 4 uptake after radioembolization. Interestingly, even in lesions with uptake lower than that in healthy liver tissue on ^{99m}Tc-MAA SPECT (grade 4), ^{90}Y-bremsstrahlung SPECT revealed that most had higher uptake after radioembolization. In particular, of the 57 lesions with grade 4 uptake on ^{99m}Tc-MAA SPECT, 12 (21.1%) had grade 1 uptake and 26 (45.6%) grade 2 uptake on ^{90}Y-bremsstrahlung SPECT, whereas only 3 (5.3%) and 16 (28.1%) had grade 3 and 4 uptake, respectively.

In accordance with the uptake pattern on ^{99m}Tc-MAA SPECT, most tumors had grade 2 uptake on ^{90}Y-bremsstrahlung SPECT (Table 1). In an analysis of tumor primary, the highest rates for grade 2 uptake were in urologic tumors (90%), malignant melanoma (83.3%), HCC (72.7%), and CRC (72.2%). The rates for grade 1 uptake were highest for breast cancer (52.8%), NETs (46.1%), sarcoma (40%), and non-CRC gastrointestinal tumors (37.5%). These results agree strongly with the findings from ^{99m}Tc-MAA SPECT. The rates for lower uptake than in normal liver tissue on ^{90}Y-bremsstrahlung SPECT (grade 4) were highest for ear-nose-throat tumors (25%) and pancreatic cancer (8.3%).

As can be assumed, mean TBR on ^{90}Y-bremsstrahlung SPECT in the 4 uptake grades differed significantly among primaries ($P < 0.001$, respectively). There were significant differences in mean TBR between ^{99m}Tc-MAA and ^{90}Y-bremsstrahlung SPECT, being lower on ^{90}Y-bremsstrahlung SPECT in all tumor entities ($P < 0.001$). The total mean TBR was 1.9 ± 1.01 on ^{99m}Tc-MAA SPECT and 1.48 ± 0.51 on ^{90}Y-bremsstrahlung SPECT ($P < 0.001$). Details on the mean TBRs are given in Table 2. We observed the highest mean TBR on ^{99m}Tc-MAA SPECT in ear-nose-throat tumors (2.61 ± 0.55) and gastrointestinal tumors (2.27 ± 1.05). The highest values

TABLE 2
Mean TBR on ^{99m}Tc-MAA and ^{90}Y-Bremsstrahlung SPECT and Spearman Correlation Coefficient

Primary tumor	*n*	Mean TBR ± SD		Spearman correlation coefficient	*P*
		^{99m}Tc-MAA	^{90}Y-bremsstrahlung		
HCC	77	2.11 ± 1.25	1.56 ± 0.50	0.398	<0.001
CCC	65	2.05 ± 0.97	1.41 ± 0.37	0.279	0.024
Breast cancer	123	1.65 ± 0.76	1.41 ± 0.47	0.308	0.001
CRC	442	1.80 ± 0.92	1.43 ± 0.49	0.22	<0.001
NETs	180	2.16 ± 1.21	1.53 ± 0.47	0.197	0.008
PAN	24	1.92 ± 1.15	1.41 ± 0.52	0.323	0.123
PUL	10	1.99 ± 0.94	1.66 ± 0.76	0.442	0.2
MM	18	1.93 ± 1.13	1.53 ± 0.78	0.094	0.711
URO	30	1.97 ± 0.94	1.71 ± 0.31	0.05	0.795
ENT	8	2.61 ± 0.55	1.63 ± 0.90	0.143	0.736
GI	16	2.27 ± 1.05	1.81 ± 0.41	0.174	0.52
SAR	15	1.73 ± 1.10	1.64 ± 1.24	0.036	0.899
Total	1,008	1.90 ± 1.01	1.48 ± 0.51	0.261	<0.001

PAN = pancreatic cancer; PUL = lung cancer; MM = malignant carcinoma; URO = urologic tumor; ENT = ear-nose-throat tumor; GI = non-CRC gastrointestinal cancer; SAR = sarcoma.

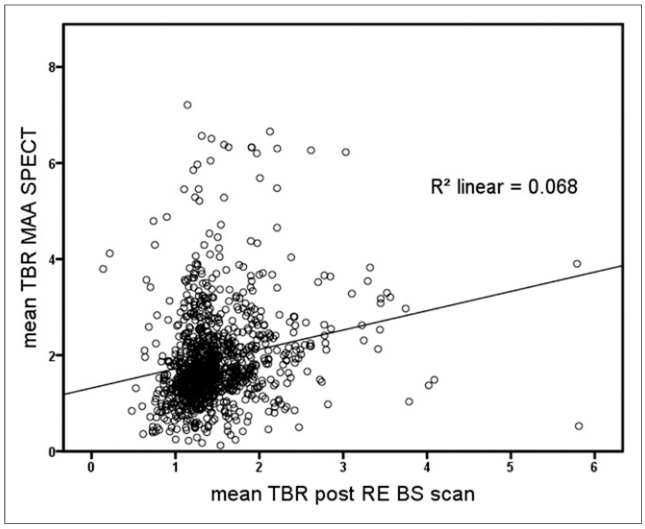

FIGURE 2. Scatterplot of mean TBR in ^{99m}Tc-MAA SPECT (*x*-axis) and mean TBR in ^{90}Y-bremsstrahlung SPECT (*y*-axis).

on ^{90}Y-bremsstrahlung SPECT were in non-CRC gastrointestinal tumors (1.81 ± 0.41) and urologic tumors (1.71 ± 0.31). The Spearman test revealed a significant correlation between ^{99m}Tc-MAA uptake and ^{90}Y-bremsstrahlung uptake in the total population ($r = 0.26$; $P < 0.001$) and in HCC ($r = 0.4$; $P < 0.001$), CCC ($r = 0.3$; $P < 0.05$), breast cancer ($r = 0.3$; $P < 0.001$), CRC ($r = 0.2$; $P < 0.001$), and NETs ($r = 0.2$; $P < 0.01$). However, the correlation coefficients between ^{99m}Tc-MAA and ^{90}Y-bremsstrahlung SPECT were low in all entities as shown in Table 2. The bivariate scatterplots for all lesions independently of the primary tumor are given in Figure 2.

Tumor vascularization remains important in terms of radioembolization. In an additional analysis, we focused on the differences in highly vascularized tumors such as HCC, CCC, and NETs and moderately vascularized tumors such as CRC and breast cancer. In accordance with the initial findings, most lesions showed high tracer accumulation in the visual interpretation regardless of tumor vascularization. More than 26% of the highly vascularized lesions had grade 1 uptake, and most of the lesions had grade 2 uptake (66.5%). The results were similar in moderately hypervascularized tumors. More than 21% had grade 1 uptake, and more than 71% had grade 2 uptake. The mean TBR revealed statistically significant higher tracer accumulation ($P < 0.01$) in highly vascularized tumors with grade 1 (2.32 ± 1.10) and grade 2 uptake (2.20 ± 1.16) than in moderately hypervascularized tumors (1.91 ± 0.88 and 1.81 ± 0.87, respectively) (Table 3).

DISCUSSION

^{99m}Tc-MAA angiography and imaging are obligatory in the workup of patients presenting for radioembolization and are implemented in procedure guidelines (*6*). On the one hand, pretherapeutic angiography is mandatory for the assessment of anatomic variations and coiling of potential aberrant vessels. On the other hand, ^{99m}Tc-MAA mimics the distribution of ^{90}Y-microspheres and is used for the evaluation of liver–lung shunting. The partition model as presented by Ho et al. implies tracer accumulation on ^{99m}Tc-MAA SPECT for dose calculations in radioembolization (*9*). This method is accepted as the most accurate yet most complex approach (*10*). However, the predictive value of ^{99m}Tc-MAA SPECT on tumor response and patient survival remains controversial. In our workgroup, previous studies on CCC patients treated with radioembolization showed a trend toward an inverse correlation between high tracer accumulation on ^{99m}Tc-MAA scintigraphy and patient survival (*7*). This seems rather surprising, as one would assume that high uptake of ^{90}Y-microspheres results in a better response to therapy. A retrospective study by Ulrich et al. on patients with CRC liver metastases found no significant correlation between ^{99m}Tc-MAA uptake and response to radioembolization as measured with ^{18}F-FDG PET (*13*). The conclusion, however, was not to exclude patients with low uptake on ^{99m}Tc-MAA scintigraphy from radioembolization, as patients with initially low ^{99m}Tc-MAA uptake also showed a significant response to therapy. These findings are in accordance with our current results.

Recently, we presented data on ^{99m}Tc-MAA tumor uptake in patients with various primary and secondary liver tumors transferred to our institution for radioembolization (*11*). Most patients with liver metastases had tumor uptake higher than that in normal liver tissue (>90% grades 1 and 2), whereas less than 8% had uptake equal to or lower than that in normal liver tissue (grades 3 and 4). Interestingly, most of these lesions with lower uptake

TABLE 3
Mean TBR and Grade in Comparison of Highly and Moderately Hypervascularized Tumors on ^{99m}Tc-MAA and ^{90}Y-Bremsstrahlung SPECT

	^{99m}Tc-MAA				^{90}Y-bremsstrahlung			
Hypervascularized…	Grade	*n*	%	Mean TBR ± SD	Grade	*n*	%	Mean TBR ± SD
Highly (*n* = 322; HCC, CCC, NETs)	1	84	26.1	2.32 ± 1.10	1	120	37.3	1.54 ± 0.41
	2	214	66.5	2.20 ± 1.16	2	187	58.1	1.54 ± 0.47
	3	6	1.9	1.24 ± 0.39	3	8	2.5	0.96 ± 0.21
	4	18	5.6	0.61 ± 0.24	4	7	2.2	0.78 ± 0.17
Moderately (*n* = 565; CRC, breast cancer)	1	121	21.4	1.91 ± 0.88	1	167	29.6	1.50 ± 0.52
	2	404	71.5	1.81 ± 0.87	2	372	65.8	1.42 ± 0.46
	3	9	1.6	1.02 ± 0.28	3	10	1.8	1.13 ± 0.24
	4	31	5.5	0.76 ± 0.23	4	16	2.8	0.86 ± 0.14

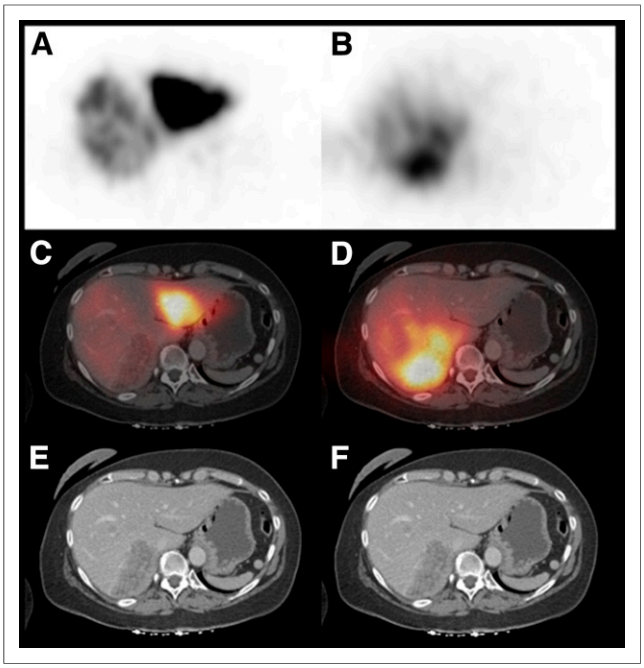

FIGURE 3. Coregistered diagnostic CT, ^{99m}Tc-MAA SPECT, and ^{90}Y-bremsstrahlung SPECT scans of 60-y-old woman with hepatically metastasized breast cancer who had undergone sequential lobar radioembolization. Hepatic lesion in right lobe (E and F) does not show relevant uptake on ^{99m}Tc-MAA SPECT (A and C). ^{90}Y-bremsstrahlung SPECT (B and D), however, reveals high uptake in tumor during radioembolization.

had high uptake on ^{90}Y-bremsstrahlung SPECT. Of the 57 lesions with grade 3 or 4 uptake, 68% had grade 1 or 2 uptake on ^{90}Y-bremsstrahlung SPECT whereas only 32% had grade 3 or 4 uptake. Thus, more than two thirds of lesions that would not have been eligible for radioembolization according to the results of ^{99m}Tc-MAA SPECT showed a relevant and measurable accumulation of ^{90}Y-microspheres. This implies that patients with low uptake on pretherapeutic imaging should not be excluded from therapy. An example is shown in Figure 3: an 81-y-old patient with CCC who had undergone sequential lobar radioembolization in our department. The tumor in the right lobe showed no relevant uptake of ^{99m}Tc-MAA and had been classified as grade 4 in the visual scoring. After radioembolization, however, ^{90}Y-bremsstrahlung SPECT revealed high uptake of ^{90}Y-microspheres.

The quantitative values, on the other hand, have to be considered carefully. The mean TBRs in this patient were 0.89 on ^{99m}Tc-MAA SPECT and 1.29 on radioembolization, which indicates uptake higher than in normal liver tissue, or grade 2. The distribution of ^{90}Y-microspheres was heterogenous in liver tissue, with no evidence of tumor on the diagnostic CT scan. This represents a limitation of TBR, as there might be a heterogenous distribution of ^{90}Y-microspheres in some patients. Diagnostic information from CT and MR scans is mandatory to differentiate tumor-associated tracer accumulation. Nevertheless, the position of the region of interest in the normal liver tissue can bias the results. Furthermore, the distribution of ^{90}Y-microspheres can also be inhomogeneous in the tumor itself. A tissue specimen from a patient with CRC liver metastasis revealed a higher accumulation of ^{90}Y-microspheres in the tumor periphery than in the center (*14,15*).

Maximum TBRs were not analyzed in this study. In our previous work, maximum TBRs calculated by dividing the maximum counts per pixel of tumor from the mean counts per pixel of normal liver tissue showed a high SD (4.8 ± 4.1) and a wide range (0.2–50.1) (*11*). Because counting rates in single pixels might be higher, maximum TBR is prone to outlier effects.

Correlations of ^{99m}Tc- and ^{90}Y-microsphere uptake relying on segmental TBRs in the liver might be less susceptible to outliers. When comparing segmental distribution of ^{99m}Tc-MAA and ^{90}Y-microspheres, however, Wondergem et al. discovered only a poor prediction of intrahepatic ^{90}Y-microsphere uptake from ^{99m}Tc-MAA SPECT (*16*). The difference was less in segments with higher tumor involvement, indicating that the distribution of ^{99m}Tc-MAA and ^{90}Y-microspheres in normal liver tissue is not always homogeneous and comparable. One of the reasons might be the difference in particle sizes between ^{99m}Tc-MAA and ^{90}Y-microspheres, which are comparable but not identical (~10–50 μm and 20–60 μm, respectively). Another reason could be the catheter tip position. Most centers recommend use of the same catheter tip position during ^{99m}Tc-angiography and radioembolization. Wondergem et al. found significant differences in ^{99m}Tc-MAA and ^{90}Y-microsphere distribution when there was suboptimal agreement in the position of the catheter tip between the two procedures (*16*). In a lesion-based analysis Ulrich et al., on the other hand, found no significant impact of different catheter tip positions on treatment response assessed by changes in tumor diameter (*13*). Finally and probably most important, the embolizing effect of ^{90}Y-microspheres, which lack ^{99m}Tc-MAA, is likely to influence distribution during the course of radioembolization.

Quantification of uptake remains difficult. We identified a significant correlation in TBRs between ^{99m}Tc-MAA and ^{90}Y-bremsstrahlung SPECT. Nevertheless, the correlation was only weak ($r = 0.26$), with significantly higher values on ^{99m}Tc-MAA than on ^{90}Y-bremsstrahlung SPECT, probably due in part to the poor image quality of ^{90}Y-bremsstrahlung SPECT. A voxelwise quantification of tracer accumulation and the calculation of TBRs might be susceptible for single voxels with higher or lower values. Various conditions, such as catheter tip position and prior therapies (e.g., angiogenesis inhibitors), can interfere with the distribution of ^{90}Y-microspheres within the tumor and the normal liver tissue. Interestingly, though, mean TBRs were lower on ^{90}Y-bremsstrahlung than on ^{99m}Tc-MAA SPECT, whereas the SDs of mean TBRs were lower on ^{90}Y-bremsstrahlung than on ^{99m}Tc-MAA SPECT. The difference in particle size, the embolizing effect of ^{90}Y-microspheres, and the inhomogeneous tracer distribution in normal liver tissue might be reasons for these findings. New developments in assessing the result of radioembolization, and posttherapeutic dosimetry such as ^{90}Y PET investigations, are likely to overcome these shortcomings of ^{90}Y-bremsstrahlung SPECT. Several workgroups have highlighted the advantages of posttherapeutic ^{90}Y PET as compared with ^{90}Y-bremsstrahlung SPECT (*17,18*). Nevertheless, especially in a clinical setting the visual interpretation of uptake seems to be favorable, bearing in mind that most patients in our study with low uptake on ^{99m}Tc-MAA SPECT showed high uptake of ^{90}Y-microspheres on ^{90}Y-bremsstrahlung SPECT.

The partition model is considered the superior method in terms of dosimetry and dose calculation for radioembolization. In a recent study, Garin et al. presented encouraging results on patients with HCC who had undergone radioembolization according to dose calculation derived from ^{99m}Tc-MAA SPECT data (*19*). ^{99m}Tc-MAA SPECT was highly predictive of tumor response according to the criteria of the

European Association for the Study of the Liver. However, evaluation was difficult in lesions of high mass with central necrosis or heterogeneous uptake. The closer correlation to ^{99m}Tc-MAA uptake in that study might be explained by the TheraSphere (Theragenics Corp.) ^{90}Y-microspheres that were used, which have a much less embolizing effect. On the basis of these difficulties, most study groups recommend additional qualitative and visual analysis before interpreting data.

CONCLUSION

We identified a significant but weak correlation in mean TBRs between ^{99m}Tc-MAA SPECT and ^{90}Y-microsphere uptake after radioembolization in a large number of patients with different primary tumors. Visual grading of tracer distribution revealed that lesions with high uptake on ^{99m}Tc-MAA SPECT maintained high uptake of ^{90}Y-microspheres during radioembolization. More than 60% of lesions with lower uptake than in healthy liver tissue before therapy also had high uptake after therapy. Thus, patients with low uptake on pretherapeutic ^{99m}Tc-MAA imaging should not be excluded from radioembolization.

DISCLOSURE

The costs of publication of this article were defrayed in part by the payment of page charges. Therefore, and solely to indicate this fact, this article is hereby marked "advertisement" in accordance with 18 USC section 1734. No potential conflict of interest relevant to this article was reported.

REFERENCES

1. Verslype C, Rosmorduc O, Rougier P, Group EGW. Hepatocellular carcinoma: ESMO-ESDO clinical practice guidelines for diagnosis, treatment and follow-up. *Ann Oncol.* 2012;23(suppl 7):vii41–vii48.
2. Van Cutsem E, Cervantes A, Nordlinger B, Arnold D, Group EGW. Metastatic colorectal cancer: ESMO clinical practice guidelines for diagnosis, treatment and follow-up. *Ann Oncol.* 2014;25(suppl 3):iii1–iii9.
3. Pavel M, Baudin E, Couvelard A, et al. ENETS consensus guidelines for the management of patients with liver and other distant metastases from neuroendocrine neoplasms of foregut, midgut, hindgut, and unknown primary. *Neuroendocrinology.* 2012;95:157–176.
4. Michl M, Haug AR, Jakobs TF, et al. Radioembolization with yttrium-90 microspheres (SIRT) in pancreatic cancer patients with liver metastases: efficacy, safety and prognostic factors. *Oncology.* 2014;86:24–32.
5. Xing M, Prajapati HJ, Dhanasekaran R, et al. Selective internal yttrium-90 radioembolization therapy (^{90}Y-SIRT) versus best supportive care in patients with unresectable metastatic melanoma to the liver refractory to systemic therapy: safety and efficacy cohort study. *Am J Clin Oncol.* August 7, 2014 [Epub ahead of print].
6. Giammarile F, Bodei L, Chiesa C, et al. EANM procedure guideline for the treatment of liver cancer and liver metastases with intra-arterial radioactive compounds. *Eur J Nucl Med Mol Imaging.* 2011;38:1393–1406.
7. Haug AR, Heinemann V, Bruns CJ, et al. ^{18}F-FDG PET independently predicts survival in patients with cholangiocellular carcinoma treated with ^{90}Y microspheres. *Eur J Nucl Med Mol Imaging.* 2011;38:1037–1045.
8. Flamen P, Vanderlinden B, Delatte P, et al. Multimodality imaging can predict the metabolic response of unresectable colorectal liver metastases to radioembolization therapy with yttrium-90 labeled resin microspheres. *Phys Med Biol.* 2008;53:6591–6603.
9. Ho S, Lau WY, Leung TW, et al. Partition model for estimating radiation doses from yttrium-90 microspheres in treating hepatic tumours. *Eur J Nucl Med.* 1996;23:947–952.
10. Cremonesi M, Chiesa C, Strigari L, et al. Radioembolization of hepatic lesions from a radiobiology and dosimetric perspective. *Front Oncol.* 2014;4:210.
11. Ilhan H, Goritschan A, Paprottka P, et al. Systematic evaluation of tumoral ^{99m}Tc-MAA uptake using SPECT and SPECT/CT in 502 patients before ^{90}Y radioembolization. *J Nucl Med.* 2015;56:333–338.
12. Sabet A, Ahmadzadehfar H, Muckle M, et al. Significance of oral administration of sodium perchlorate in planning liver-directed radioembolization. *J Nucl Med.* 2011;52:1063–1067.
13. Ulrich G, Dudeck O, Furth C, et al. Predictive value of intratumoral ^{99m}Tc-macroaggregated albumin uptake in patients with colorectal liver metastases scheduled for radioembolization with ^{90}Y-microspheres. *J Nucl Med.* 2013;54:516–522.
14. Campbell AM, Bailey IH, Burton MA. Analysis of the distribution of intra-arterial microspheres in human liver following hepatic yttrium-90 microsphere therapy. *Phys Med Biol.* 2000;45:1023–1033.
15. Campbell AM, Bailey IH, Burton MA. Tumour dosimetry in human liver following hepatic yttrium-90 microsphere therapy. *Phys Med Biol.* 2001;46:487–498.
16. Wondergem M, Smits ML, Elschot M, et al. ^{99m}Tc-macroaggregated albumin poorly predicts the intrahepatic distribution of ^{90}Y resin microspheres in hepatic radioembolization. *J Nucl Med.* 2013;54:1294–1301.
17. Srinivas SM, Natarajan N, Kuroiwa J, et al. Determination of radiation absorbed dose to primary liver tumors and normal liver tissue using post-radioembolization ^{90}Y PET. *Front Oncol.* 2014;4:255.
18. Barber TW, Yap KS, Cherk MH, Powell A, Kalff V. Comparison of positron emission tomography/CT and bremsstrahlung imaging following Y-90 radiation synovectomy. *J Med Imaging Radiat Oncol.* 2013;57:567–571.
19. Garin E, Lenoir L, Edeline J, et al. Boosted selective internal radiation therapy with ^{90}Y-loaded glass microspheres (B-SIRT) for hepatocellular carcinoma patients: a new personalized promising concept. *Eur J Nucl Med Mol Imaging.* 2013;40:1057–1068.

JNM The Journal of NUCLEAR MEDICINE

Predictive Value of ^{99m}Tc-MAA SPECT for ^{90}Y-Labeled Resin Microsphere Distribution in Radioembolization of Primary and Secondary Hepatic Tumors

Harun Ilhan, Anna Goritschan, Philipp Paprottka, Tobias F. Jakobs, Wolfgang P. Fendler, Andrei Todica, Peter Bartenstein, Marcus Hacker and Alexander R. Haug

J Nucl Med. 2015;56:1654-1660.
Published online: August 27, 2015.
Doi: 10.2967/jnumed.115.162685

The Journal of Nuclear Medicine is published monthly.
SNMMI | Society of Nuclear Medicine and Molecular Imaging
1850 Samuel Morse Drive, Reston, VA 20190.
(Print ISSN: 0161-5505, Online ISSN: 2159-662X)

SNMMI SOCIETY OF NUCLEAR MEDICINE AND MOLECULAR IMAGING